Structure at 2.5-Å Resolution of Chemically Synthesized Human Immunodeficiency Virus Type 1 Protease Complexed with a Hydroxyethylene-Based Inhibitor[†,‡]

Mariusz Jaskólski,[§,∥] Alfredo G. Tomasselli,[⊥] Tomi K. Sawyer,[⊥] Douglas G. Staples,[⊥] Robert L. Heinrikson,[⊥] Jens Schneider,[○] Stephen B. H. Kent,[○,#] and Alexander Wlodawer*[,∥]

Macromolecular Structure Laboratory, National Cancer Institute-Frederick Cancer Research and Development Center, ABL-Basic Research Program, Frederick, Maryland 21702-1201, Biopolymer Chemistry Unit, The Upjohn Company, Kalamazoo, Michigan 49001, Division of Biology, California Institute of Technology, Pasadena, California 91125, and Graduate School of Science and Technology, Bond University, Queensland, Australia 4229

Received August 3, 1990; Revised Manuscript Received November 8, 1990

ABSTRACT: The crystal structure of a complex between chemically synthesized human immunodeficiency virus type 1 (HIV-1) protease and an octapeptide inhibitor has been refined to an *R* factor of 0.138 at 2.5-Å resolution. The substrate-based inhibitor, H-Val-Ser-Gln-Asn-LeuΨ[CH(OH)CH_2]Val-Ile-Val-OH (U-85548e) contains a hydroxyethylene isostere replacement at the scissile bond that is believed to mimic the tetrahedral transition state of the proteolytic reaction. This potent inhibitor has $K_i < 1$ nM and was developed as an active-site titrant of the HIV-1 protease. The inhibitor binds in an extended conformation and is involved in β-sheet interactions with the active-site floor and flaps of the enzyme, which form the substrate/inhibitor cavity. The inhibitor diastereomer has the *S* configuration at the chiral carbon atom of the hydroxyethylene insert, and the hydroxyl group is within H-bonding distance of the two active-site carboxyl groups in the enzyme dimer. The two subunits of the enzyme are related by a pseudodyad, which superposes them at a 178° rotation. The main difference between the subunits is in the β turns of the flaps, which have different conformations in the two monomers. The inhibitor has a clear preferred orientation in the active site and the alternative conformation, if any, is a minor one (occupancy of less than 30%). A new model of the enzymatic mechanism is proposed in which the proteolytic reaction is viewed as a one-step process during which the nucleophile (water molecule) and electrophile (an acidic proton) attack the scissile bond in a concerted manner.

An essential step in the maturation of retriviruses involves processing of the *gag* and *gag/pol* viral polyproteins by a protease (PR) that is itself encoded in the *pol* gene (Oroszlan, 1989). Because the action of this retroviral protease is indispensable for production of infective virus particles (Kramer et al., 1986; Kohl et al., 1988), the enzyme has been targeted for inhibition in therapeutic applications. In view of the current concern over the incidence and spread of acquired immunodeficiency syndrome (AIDS), special emphasis has been placed on the development of inhibitors of the protease from the human immunodeficiency virus (HIV) that might serve as drugs in the treatment of this disease.

Strategies for the rational design of HIV PR inhibitors may be considered under two broad categories. The first is based upon knowledge of the substrate specifity gained, by and large, from information concerning bonds hydrolyzed in the viral polyproteins during the maturation process (Darke et al., 1988). This approach has led to the development of a number of peptidemimetic inhibitors in which the bond normally cleaved by the HIV PR is replaced by one that is inert to hydrolysis (Richards et al., 1989; Blumenstein et al., 1989; Dreyer et al., 1989; Tomasselli et al., 1990a). For the most part, these scissile bond isosteres are the same as those used in the design of inhibitors of other aspartic proteases such as renin (cf. Greenlee, 1990). They include aminomethylene [CH_2NH], hydroxyethylamine [$CH(OH)CH_2N$], hydroxyethylene [$CH(OH)CH_2$], and diol [CH(OH)CH(OH)] groups joining selected amino acids in the P1 and P1′ positions. Numerous reports of specific HIV protease inhibitors have appeared in which the kinetics of inhibition has been evaluated against the pure recombinant or synthetic enzyme, usually from HIV-1 (Richards et al., 1989; Blumenstein et al., 1989; Dreyer et al., 1989; Rich et al., 1990; Tomasselli et al., 1990a) but also in some cases from HIV-2 (Tomasselli et al., 1990b; Richards et al., 1990; Roberts et al., 1990). The K_i values for some of these compounds are in the subnanomolar range. Moreover, a number of these inhibitors have been shown to possess antiviral activity, both in HIV-infected cell culture assays (McQuade et al., 1990; Meek et al., 1990; Roberts et al., 1990) and in cell model systems that mimic the process of infection (McQuade et al., 1990). As might be expected, antiviral potency does not always correlate with K_i; presumably, the inhibitors must be able to gain access to the cell or to the compartment in which the protease exhibits its activity. In general, however, there is some correlation between K_i and the antiviral activity, with the best antiviral compounds described thus far having K_i values in the nanomolar to subnanomolar range (Roberts et al., 1990).

The second approach to drug design follows from detailed structural information concerning the protease, both alone and complexed with inhibitors. X-ray crystallographic analyses of the HIV-1 PR (Navia et al., 1989; Wlodawer et al., 1989;

[†] Research sponsored in part by the National Cancer Institute, DHHS, under Contract N01-CO-74101 with ABL.

[‡] HIV-1 protease complex coordinates have been submitted to the Brookhaven Protein Data Bank as file 8HVP.

* To whom correspondence should be sent.

[§] On leave from A. Mickiewicz University, Faculty of Chemistry, Poznań, Poland.

[∥] NCI-Frederick Cancer Research and Development Center.

[⊥] The Upjohn Co.

[○] California Institute of Technology.

[#] Bond University.

0006-2960/91/0430-1600$02.50/0

Lapatto et al., 1989) have established that the viral enzyme is a dimer with clear structural homology to well-characterized cell-derived aspartic proteases. More recently, Miller et al. (1989b) and Swain et al. (1990) reported structures of the enzyme complexed with inhibitors with reduced peptide bond and hydroxyethylamine scissile bond replacements, respectively. Accordingly, it is now possible to delineate detailed interactions between functionalities in the inhibitor and groups in the enzyme. The present report describes the analysis of a complex of a chemically synthesized HIV-1 protease with an inhibitor containing a hydroxyethylene replacement for the scissile peptide bond. Considered together, the findings of all three crystal structures are in agreement as to the modes of inhibitor binding to the enzyme and provide important new information for de novo design of HIV protease inhibitors. Moreover, these results have allowed inferences as to particular features of the catalytic mechanism that should apply to aspartic proteases in general.

Materials and Methods

(*a*) *Synthesis and Characterization of the HIV Protease and Inhibitor.* The HIV-1 protease used in these investigations was prepared by solid-phase peptide synthesis (Schneider & Kent, 1988; Kent, 1988; Miller et al., 1989). The sequence used was that of the SF2 isolate with cysteines replaced by L-α-amino-*n*-butyric acid (Aba). The enzymatic activity of the synthetic enzyme was similar to that of the recombinant protein (Darke et al., 1988).

The synthesis of U-85548e was performed by stepwise coupling of the appropriate N^{α}-(*tert*-butyloxy)carbonyl amino acids and N^{α}-Boc-LeuΨ[CH(O-*tert*-butyldimethylsilyl)-CH_2]Val-OH on a solid-phase (Merrifield) resin. The general methods of organic and peptide synthesis, anhydrous HF cleavage, and reverse-phase HPLC purification used to obtain the desired pseudopeptidyl product were adopted from previously reported studies (Sawyer et al., 1988). The LeuΨ-[CH(OH)CH_2]Val intermediate was prepared by using chemical methods previously reported (Wuts et al., 1988), which have established *S* configuration at all of its three chiral centers. In the preparation of U-85548e we have exclusively used the N,O-protected derivative, Boc-LeuΨ[CH(O-*tert*-butyldimethylsilyl)CH_2]Val-OH, which is the 2*S*,4*S*,5*S* diastereomer. The synthesis resulted in a pure diastereomer with *S* configuration at the chiral C atom of the hydroxyethylene group. The chemical authenticity and purity of synthetic U-85548e was established by amino acid analysis, high-resolution fast atom bombardment mass spectrometry ($[M + H]^+$ at m/z 872), and analytical reverse-phase HPLC (purity >99%). The binding constant of this inhibitor to PR was recently redetermined to be <1 nM (Tomasselli et al., 1990a).

(*b*) *Crystallization and Data Collection.* The procedure used for crystallization of the complex with the U-85548e inhibitor was similar to that previously used with the reduced peptide bond inhibitor MVT-101 (Miller et al., 1989), namely, pH = 5.4, 6 mg/mL protein, and 20-fold molar excess of inhibitor. The complex crystallizes isomorphously with those containing aminomethylene- (Miller et al., 1989b) and hydroxyethylamine-based (Swain et al., 1990) inhibitors. The space group is $P2_12_12_1$ with a = 51.65 Å, b = 58.76 Å, c = 61.62 Å, and V = 187014 Å^3 and the asymmetric unit contains one protease dimer–inhibitor complex.

X-ray data were collected by using a Siemens area detector mounted on a Rigaku RU-200 rotating anode source. Two small crystals (approximate size 0.2 × 0.08 × 0.04 mm) were used to measure 25 199 individual reflections, which were reduced to 6304 unique data (out of 7114 possible to 2.47-Å resolution). The number of observed reflections [$I > 1.5\sigma(I)$] in the 10–2.5-Å shell that were used in the refinement was 4768.

(*c*) *Structure Solution and Refinement.* Since the crystals are isomorphous with those of two other HIV-1 PR–inhibitor complexes (Miller et al., 1989b; Swain et al., 1990), the starting model for the homodimeric enzyme was taken directly from the protease–hydroxyethylamine heptapeptide (JG-365) complex (Swain et al., 1990). The initial $(|F_o| - |F_c|)\alpha_c$ map obtained by using the phases calculated from protein only clearly showed the inhibitor electron density in the active-site cleft. As the scissile bond analogue (Ψ[-CH(OH)CH_2-]) of this octapeptide inhibitor is between residues 5 and 6, and, as positive electron density was seen for all residues, there was no ambiguity about the polarity of the inhibitor molecule when it was initially fit into the difference electron density map in the active site. The inhibitor model was built by using PROLSQ standard groups (Hendrickson, 1985) for sites P5–P2 and P2′–P3′ and non-standard groups for the scissile bond analogue dipeptide P1–P1′. At P1 (205Leu[OH] or Ler) a leucine reduced to an alcohol derivative (1-hydroxy-2-amino-4-methylpentylene residue) was placed and at P1′ (206Val[CH_2] or Vac) a methylene derivative of desaminovaline (2,3-dimethylbutanoic acid residue) was used. The P1–P1′ link [C(205)–C$_\tau$(206)] was defined in PROTIN (Hendrickson, 1985) as C(205)–Cτ(206) 1.53 Å, Cα(205)···Cτ(206) 2.50 Å, C(205)···Cα(206) 2.51 Å, and Oσ(205)···Cτ(206) 2.41 Å. The disposition of the substituents on the Cα chiral centers of the P1–P1′ dipeptide was modeled as in standard Leu and Val residues. The hydroxyl substituent on the new asymmetry center [C*(205)] was originally modeled in the *S* configuration but was left unrestrained in the course of the refinement.

Restrained least-squares refinement of the structure with individual isotropic temperature factors was carried out in four rounds using the PROFFT (Finzel, 1987; Sheriff, 1987) version of PROLSQ (Hendrickson, 1985). Between the least-squares minimizations the structure was manually adjusted in $(2|F_o| - |F_c|)\alpha_c$ maps [calculated with PROTEIN (Steigemann, 1974)] by using an Evans & Sutherland PS390 graphics system running FRODO (Jones, 1985). During the manual intervention sessions water molecules were located and verified subject to the criteria of good electron density and acceptable H bonding with other atoms. The structure factor weighting scheme used was of the form $w_F = \sigma_F^{-2}$ with σ_F = [30.0 − 40.0(sin (θ/λ) − 1/6)], which corresponded to $\sigma_F \approx 0.5\langle||F_o| - |F_c||\rangle$ (Table I). The rms positional shift in the last cycle of refinement was 0.004 (9) Å and the final model is characterized by an *R* factor of 0.138 and by an rms deviation between ideal and observed bond distances of 0.014 Å (Table I). The coordinates have been deposited with the Brookhaven Protein Data Bank (file 8HVP).

Results

The refined model of the HIV-1 PR–U-85548e inhibitor complex consists of 1516 enzyme atoms with $\langle B_{iso}\rangle$ = 12.3 Å^2, 61 inhibitor atoms with $\langle B_{iso}\rangle$ = 13 Å^2, and 80 water molecules, 43 of which occupy the same sites and have the same numbers (between 301 and 395) as their counterparts in the HIV-1 PR–JG-365 structure (Swain et al., 1990). The remaining water molecules are numbered 401–437 in the order of their isotropic temperature factors.

The protein is a homodimeric molecule, made up of two 99-residue polypeptide chains with approximate dimensions of 45 × 23 × 25 Å. The single substrate-derived inhibitor molecule is bound as an extended chain in a 23-Å-long groove

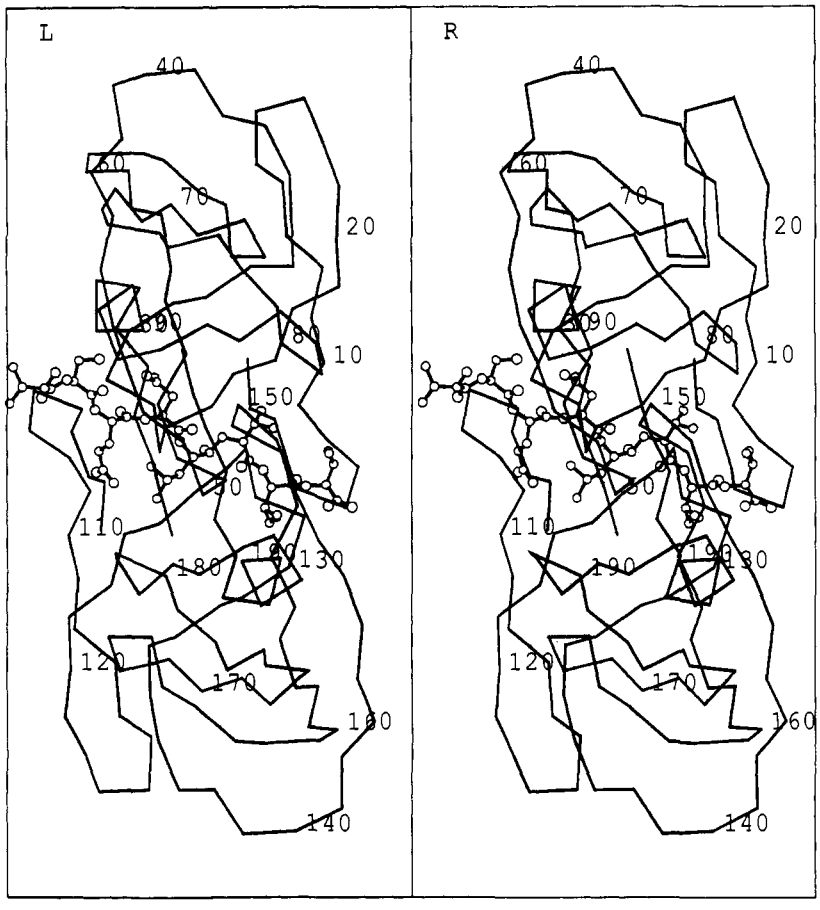

FIGURE 1: Stereoview of the HIV-1 PR–U-85548e complex. The protease is represented as a C_α skeleton and the inhibitor bound in the active site as ball-and-stick model.

Table I: Refinement Statistics of the Final Model

R factor	0.138
weights	$w = \sigma_F^{-2}$
with	$\sigma_F = (30.0) + (-40.0)(s - 1/6)$
resolutn	10.0–2.5 Å
no. of reflectns	4768
no. of atoms	1646
Root Mean Square Deviations from Ideality[a]	
dist restraints	
bond dist	0.014 (0.018) Å
angle dist	0.053 (0.035) Å
planar 1–4 dist	0.067 (0.050) Å
plane restraints	0.020 (0.025) Å
chiral center restraints	0.179 (0.150) Å^3
nonbonded restraints	
single-torsion contact	0.217 (0.300) Å
multiple-torsion contact	0.264 (0.300) Å
possible (X···Y) H bond	0.306 (0.300) Å
conformational torsion angles	
planar	3.7° (4.0°)
staggered	20.0° (10.0°)
orthonormal	18.2° (30.0°)
B_{iso} restraints	
main-chain bond	2.45 (3.00) Å^2
main-chain angle	3.58 (3.50) Å^2
side-chain bond	6.24 (5.00) Å^2
side-chain angle	8.63 (8.00) Å^2
H bond	12.01 (25.00) Å^2

[a] Target restraints in parentheses.

running across the dimer interface on one side of the molecule (Figure 1). The two "flaps", one from each monomer and each made up of several residues of an antiparallel β strand joined by a β turn around Ile50 (150)–Gly51 (151), are closed over part of the inhibitor, desolvating the central residues around the scissile bond surrogate. The flaps are much closer to the body of the enzyme than in the structure without the inhibitor (Wlodawer et al., 1989) and interact with the inhibitor via H bonding through a single well-defined water molecule (Wat301) and through other H bonds and hydrophobic interactions. The catalytically essential Asp25 and Asp125 side chains are found at the scissile bond isostere, on the other side of the inhibitor, away from the flaps. These side chains interact directly with the OH group of the scissile bond isostere.

The main-chain ϕ/ψ angles are clustered in the allowed regions of the Ramachandran plot (Figure 2), the several outliers being mostly glycines. The average temperature factors along the polypeptide chain are the highest at the surface loops 115–118, 138–142, and 168–170 (all located in close proximity on the molecular surface) in monomer II (Figure 3). In monomer I, the loops 15–18 and 68–70 show much lower thermal motion. This result is difficult to explain as in the crystal packing each of those loops in monomer I has the corresponding loop in monomer II from another, symmetry-related, enzyme molecule as its near neighbor.

When the protein structure from the present study is compared with that in another HIV-1 PR–inhibitor complex (Swain et al., 1990), the main-chain atoms of the two dimers can be superimposed at an rms deviation of 0.38 Å for 777 (out of 792) atom pairs. The only significant difference between these two models of HIV-1 PR is in the 115–118 tight β turn of monomer II which in the HIV-1 PR–JG-365 complex has been modeled as type I (Richardson, 1981). The present structure has this turn in type II conformation in both subunits. As this turn is located on the surface of the molecule and is characterized by high thermal motion (Figure 3), no definite answer is possible to resolve this discrepancy.

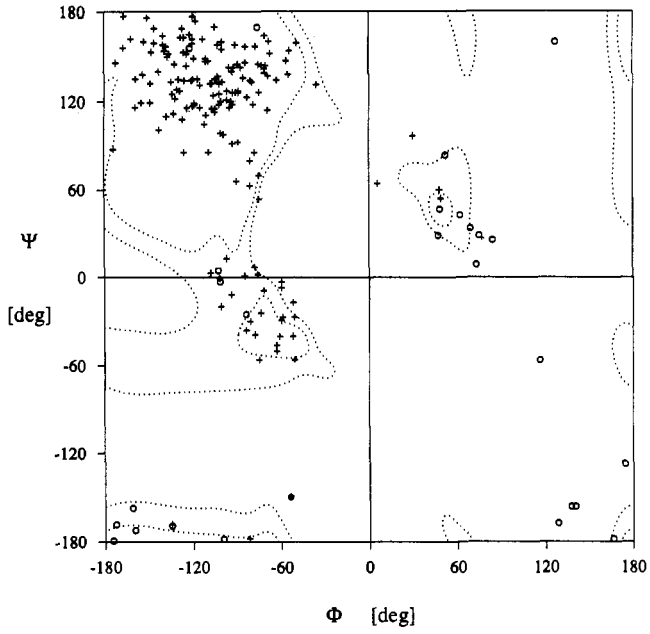

FIGURE 2: Ramachandran ϕ/ψ plot (Ramachandran & Sasisekharan, 1968) for the protein part of the complex. Circles (O) mark glycine and crosses (+) all other residues. The isoenergy contours correspond to 4 and 8 kcal/mol levels in the conformational map of alanine dipeptide (Peters & Peters, 1981).

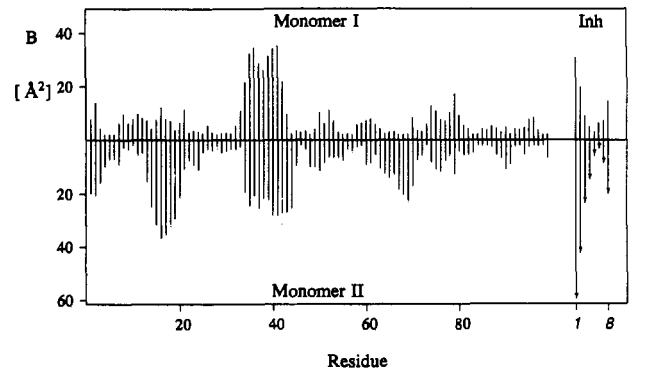

FIGURE 3: Isotropic temperature factors averaged over the main-chain atoms at each residue in monomer I (top) and in monomer II (bottom). In the inhibitor section (Inh), the top bars correspond to the results of the refinement with the inhibitor in the major orientation and the lower arrows correspond to the results of the refinement with the inhibitor in a possible minor orientation (see text).

The two monomers composing the dimeric enzyme are related by a pseudodyad approximating the true crystallographic symmetry of the unliganded enzyme (Wlodawer et al., 1989) in a way similar to that reported for other HIV-1 PR–inhibitor complexes (Miller et al., 1989b; Swain et al., 1990). The pseudo-2-fold axis of the complex is very close to the [011] direction. For the principal dimer in the unit cell, it is located exactly in the *b*,*c* plane and makes an angle of only 6° with the (*b* + *c*) diagonal in this plane. The two subunits superimpose at a 178° rotation with an rms deviation of 0.61 Å for 392 (out of 396) of their main-chain atom pairs. When all atoms are used for alignment, the rotation is also 178° and the monomers superimpose at an rms deviation of 0.69 Å for 679 (out of 758) atom pairs. It is interesting to note that the crystallographically independent subunits of the dimer of Rous sarcoma virus (RSV) protease in its native structure are also related by a 178° rotation (Jaskólski et al., 1990).

Figure 4 shows the deviations between the corresponding atoms of monomer I and monomer II averaged at each residue over the main-chain and side-chain atoms after least-squares alignment of their main-chain atoms. The largest deviations

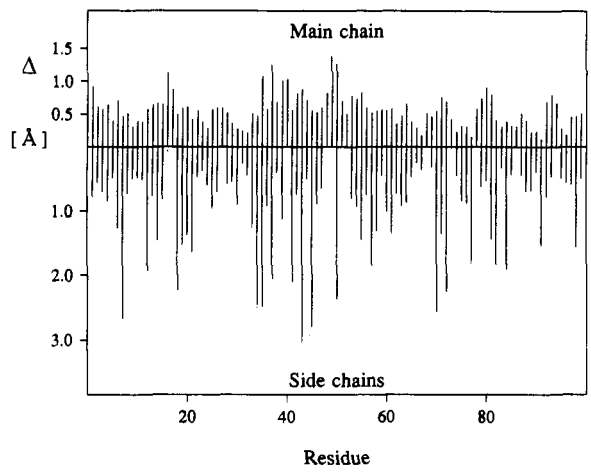

FIGURE 4: Average deviations between corresponding atoms of the two monomers after least-squares alignment of their main-chain atoms.

between the side chains of the two monomers in Figure 4 correspond to long-side-chain residues located in surface loops. For the main chain, the largest discrepancies correspond to loop and turn regions and correlate very well with the temperature factor distribution in Figure 3. An additional region of difference is at residues 49–50 (149–150 in monomer II) near the tip of the flap. The native dimer symmetry is disturbed here as the flap arms close over the inhibitor in the active site (Wlodawer et al., 1989; Miller et al., 1989b; Swain et al., 1990). With the inhibitor (and probably also substrate) in the catalytic cleft, the flaps are not only pulled toward the active site but also reorient their β-turn tips and lock tightly over the bound molecule. This lock is provided by a main-chain Gly51 N···O=C Ile150 hydrogen bond. In contrast, the C=O group on the complementary flap (Ile50) points outward, thus violating the local symmetry (Figures 5 and 6).

The breakdown of the dimer symmetry at the tips of the flaps can be correlated with the asymmetry of an oligopeptide inhibitor in the active site cleft. Figure 6 illustrates the topography of a complex between an asymmetric inhibitor and the homodimeric retroviral protease. The direction of the oligopeptide chain of the inhibitor is not perpendicular to the long axis of the dimer (running from monomer I to monomer II across the active site). The inclination is quite appreciable and places the inhibitor at such an angle relative to the flaps at which flap···inhibitor β sheets can be formed (see below). Figure 6 represents the topography of the present complex with the orientation of the inhibitor corresponding to the initial fit to the electron density map. At this orientation, the N terminus of the inhibitor is proximal to that monomer (I) which has the Ile50 C=O group pointing away from the complementary flap. The topography of the HIV-1 PR–JG-365 complex is identical (Swain et al., 1990).

The nearly symmetric structure of the protease dimer found in this study suggests, however, that the possibility of placing the inhibitor in two orientations in the active site should be investigated. As mentioned above, the original placement of the inhibitor in its electron density was unambiguous but in the course of the refinement a water molecule was found near the P3′ site (Figure 5) and the electron density at the side chain of residue P5 became weaker than that corresponding to the rest of the inhibitor (Figure 7). A recent study of the complexes between acetylpepstatin and HIV-1 PR suggests that those inhibitors display orientational disorder (Fitzgerald et al., 1990). Also, the results of a refinement with 2-Å resolution data indicated that, in variance with the original report by Miller et al. (1989b), the MVT-101 inhibitor is disordered in

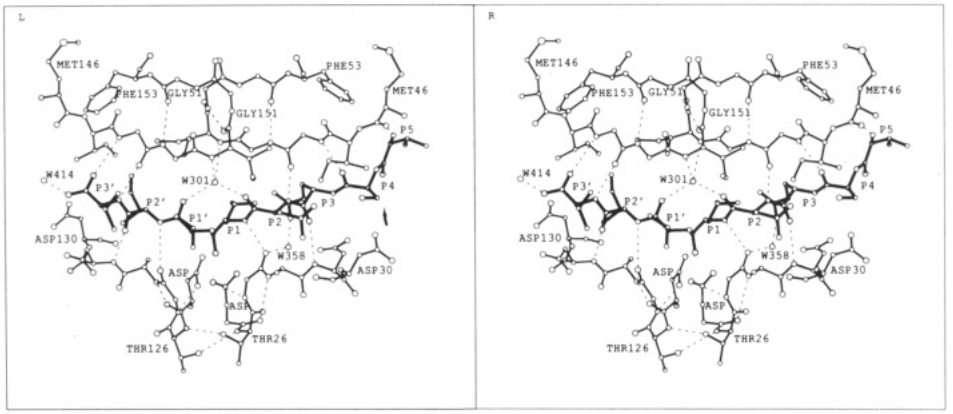

FIGURE 5: Stereoview of the inhibitor in the active site. The inhibitor is shown by a heavy line while those parts of the enzyme that form the catalytic cavity are represented by thin lines. Major H bonds are indicated by broken lines, while dotted lines represent short contacts of the inhibitor OH group with the active site.

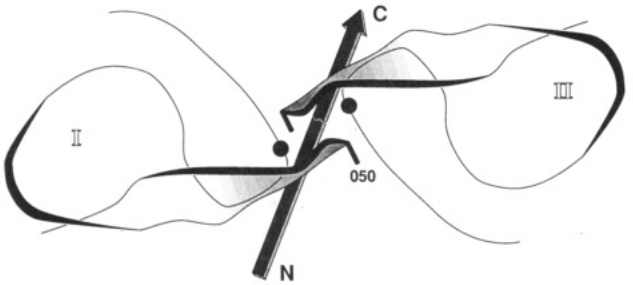

FIGURE 6: Topography of the homodimeric HIV-1 PR complexed with an asymmetric inhibitor. The polarity of the inhibitor molecule (N→C) represents the orientation prevailing in the present complex.

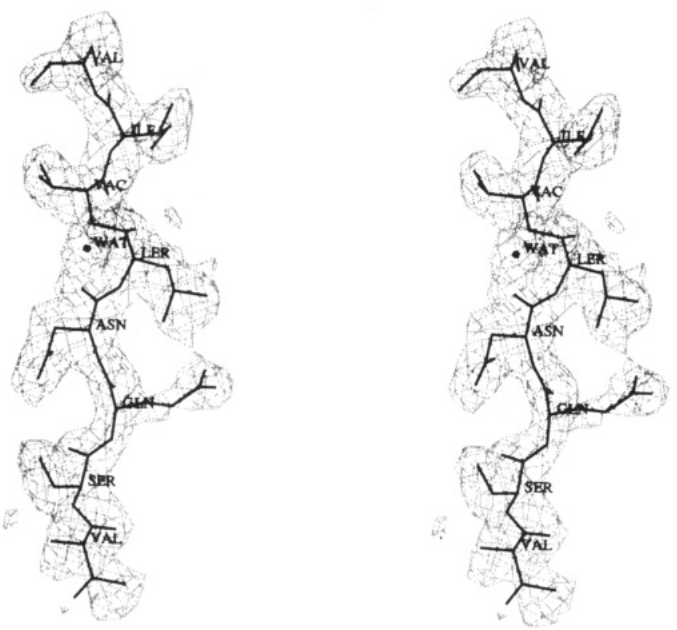

FIGURE 7: Stereoview of the inhibitor molecule in its $2|F_o| - |F_c|$ electron density map contoured at the 0.85σ level. The position of the Wat301 molecule is also marked.

its complex with HIV-1 PR (Miller et al., unpublished results).

To investigate the possibility of inhibitor disorder in the present complex, an experiment was carried out in which the dimer pseudosymmetry was applied to the refined inhibitor molecule. The dimer dyad passes nearly along the inhibitor C(205)–OH bond and through the characteristic water molecule (W301, Figure 5) and therefore these crucial elements in the catalytic cleft remain unchanged upon the rotation. The main chain of the inhibitor in the new orientation fits quite well the electron density in the common P3–P3′ segment but, obviously, its zigzag skeleton traces a different path (Figure 8). However, the carbonyl O atoms of the two molecules occupy nearly the same positions with an rms deviation of 0.63 Å for seven atom pairs [including the hydroxyl O(205) atoms]. The corresponding rms deviations for other atom types are C 0.70 Å (seven atom pairs), C_α 0.88 Å (six pairs), and C_β 1.17 Å (six pairs). For N this number is as high as 1.63 Å (six pairs) and in fact the N atoms of the main chain in one orientation fall nearly half-way between those in the other orientation (Figure 8).

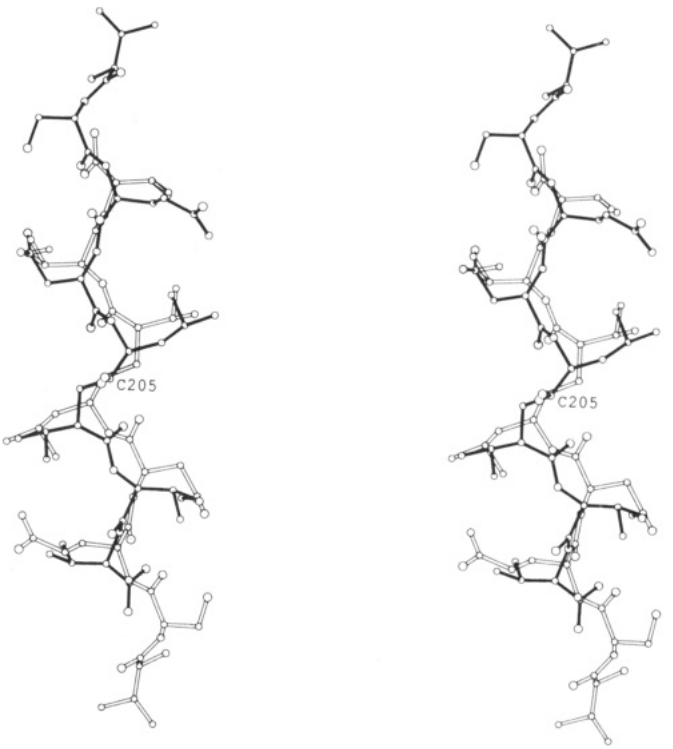

FIGURE 8: Stereoview of the refined model of the inhibitor in the major orientation (full bonds) and its image obtained through the non-crystallographic dimer symmetry (open bonds).

In the next step, the alternative inhibitor orientation was included in the least-squares refinement. However, as the currently used programs are not well designed for simultaneous refinement of alternate peptide chains (Smith et al., 1988) and as the present diffraction data cannot resolve overlapping chains, a simplified approach was used. This consisted of

refining the complex with the inhibitor in the second orientation by using the same conditions as for the initial orientation. This second refinement converged with practically identical statistical parameters and with $R = 0.141$ (versus 0.138). The main chain of the P3–P3′ segment of the new model had very good electron density but both the $2|F_o| - |F_c|$ and $|F_o| - |F_c|$ maps showed very strong, contiguous, and well-defined density corresponding to two residues beyond site P3′. The presence of this density indicates that placing the inhibitor in the second orientation alone does not account for all the information contained in the diffraction data. Careful examination of the electron density maps around the tips of the flaps (which together with a uniquely oriented inhibitor would violate the complex symmetry) did not indicate any possibility of disorder in this part of the protein.

These two observations would seem to provide evidence against inhibitor disorder. On the other hand, the inhibitor in the alternative orientation would form the same principal H bonds with the enzyme and in particular would participate in identical β-sheet interactions as the other alternative, and thus the disorder cannot be ruled out on the basis of hydrogen-bonding arguments alone. An analysis of the temperature factors of the inhibitor is more helpful. Figure 3 shows that the temperature factors of the inhibitor in the second orientation are higher than those in the first model. As in both refinements the occupancies of the inhibitor atoms were fixed at 1.0, the inhibitor temperature factors in Figure 3 can be used to roughly estimate the ratio of the two orientations (k_1:k_2) since, when the diffraction data belong to a limited shell, the approximation $k_1:k_2 \approx \exp[(B_2 - B_1)s^2]$ can be used. If most of the observations are assumed to be centered around $d = 3$ Å and $B_2 - B_1$ is used for the nonoverlapping residues (P5, P4) as 30 Å^2, $k_1:k_2$ can be estimated as 2.3:1. This demonstrates that the second orientation of the inhibitor could be at most a minor one with a population factor of no more than 30%. This low occupancy along with the arguments discussed above makes a precise analysis of this minor component impossible. All further discussion will be, therefore, based on the results obtained for the major (or only) orientation of the inhibitor molecule. It has to be realized, however, that the accuracy of these results may be somewhat lowered as the model was refined without including the possible minor component in the crystal lattice.

Figure 7 represents the inhibitor in the $2|F_o| - |F_c|$ map. The electron density is well defined along the main chain and side chains except for a small fragment of the side chain of the first residue (Val201, site P5). This residue also shows the highest thermal vibrations in the inhibitor molecule (Figure 3). These facts are explained when one compares the length of the inhibitor molecule before the scissile bond (P5–P1) with the extent of the binding cleft where it is attached: the first inhibitor residue (P5) projects outside the enzyme boundary (Figures 1 and 5) and has only marginal interactions with the protease.

The new asymmetric center [C*(205)] at the scissile bond analogue of the refined inhibitor model has the *S* configuration. This result is unbiased as the chiral volume of that atom has not been restrained in the refinement. When similar inhibitors were used with pepsin-like aspartic proteases, it were the *S* diastereomers that were preferentially bound by the enzymes and that were invariably found in the active sites of the complexes in the crystals (Blundell et al., 1987). The configuration of the analogous hydroxymethylene chiral center of the inhibitor in the HIV-1 PR–JG-365 complex has also been established as *S* (Swain et al., 1990).

Table II: Torsion Angles (deg) Characterizing the Inhibitor Main-Chain Conformation[a]

subsite	ϕ	ψ	ω
P5		11	175
P4	−106	126	178
P3	−108	148	−177
P2	−138	101	−178
P1	−97	**63**	**133**
P1′	**−56**	150	173
P2′	−139	124	177
P3′	−126	157	

[a] Torsion angles for the scissile bond surrogate are bold typed.

Table III: Geometry of the H Bonds around Wat301

H bond dist (Å)		angles (deg)	
O301···O204	2.47	O204···O301···O206	121
O301···O206	2.58	O204···O301···N50	104
O301···N50	3.35	O204···O301···N150	105
O301···N150	3.59	O206···O301···N50	121
		O206···O301···N150	109
		N50···O301···N150	92

However, in a recent paper Roberts et al. (1990) reported that for short inhibitors more stable complexes with HIV-1 PR are formed when the OH substituent at the hydroxyethylene analogue of the scissile bond is in a configuration corresponding to the *R* diastereomer. Those findings clearly do not apply to the inhibitors mentioned above. Another proof that when binding CHOH-containing inhibitors the enzyme will preferentially select those whose configuration allows for the association of the OH group with the active site has been provided by a recent study of an HIV-1 PR–$(Dip)_2$CHOH complex in which the C_2 symmetric inhibitor is composed of two "N-terminal" dipeptides (Dip) connected to a common CHOH group (Erickson et al., 1990). The hydroxymethylene C atom is not chiral and yet the inhibitor was bound in the active site with the OH group residing between the aspartates in a fashion typical of *S* inhibitors.

The inhibitor has an extended conformation and the main-chain torsion angles are listed in Table II. The pseudo-ω angle of residue P1 [C_α(205)–C(205)–CH_2(206)–C_α(206)] has a value (133°) indicating an appreciable strain around the P1–P1′ bond. Ideally, this Csp^3–Csp^3 torsion angle should be ±60 or 180°. In the present case it is only ca. 15° away from eclipse orientation but it is interesting to note that all these eclipse positions are with C–H bonds. In the case of a real peptide bond (as in a substrate), this ω torsion angle would ideally have a value of 180°. Viewed in an alternative way, the present value may represent a deformation of the scissile bond ω angle necessary for proper attachment of the inhibitor/substrate molecule in the catalytic cleft. A similar deformation of the P1–P1′ ω angle (142°) was observed in the structure of the HIV-1 PR complexed with an inhibitor with a reduced peptide bond, CH_2–N (Miller et al., 1989b), as well as in the structures of inhibitors of pepsin-like aspartic proteases (Suguna et al., 1987; Blundell et al., 1987).

Discussion

Analysis of short contacts between the inhibitor and the enzyme (Figure 5) defines several binding pockets on the enzyme corresponding to each of the inhibitor residues. Residue P5 has no specific binding pocket in the catalytic cleft (Figures 1 and 5) and makes only two contacts with the enzyme through its N(Val201) atom, whereas the bulk of the P5 side chain is outside the enzyme boundary (see above). The remaining residues (P4–P3′) are in binding pockets (S4–S3′)

Table IV: Potential H Bonds Involving the Inhibitor Molecule

inhibitor subsite	inhibitor residue: main chain	inhibitor residue: side chain	enzyme residue: main chain	enzyme residue: side chain	water	dist (Å)
P5 (Val)	N(201)		O(46)			3.73
P4 (Ser)	O(202)		N(48)			3.07
		OG(202)		OD2(30)		2.61
P3 (Gln)	N(203)			OD2(29)		3.86
	O(203)		N(29)			3.22
	O(203)				O(358)	3.62
		OE1(203)			O(358)	2.76
P2 (Asn)	N(204)		O(48)			2.68
	O(204)				O(301)	2.47
		ND2(204)	N(29)			3.21
		ND2(204)	N(30)			3.61
		ND2(204)	O(30)			3.42
P1 (Leu-[OH])	N(205)		O(27)			3.36
	OS(205)			OD1(25)		2.41
	OS(205)			OD2(25)		2.87
	OS(205)			OD1(125)		3.07
	OS(205)			OD2(125)		2.72
P1′ (Val-[CH_2])	O(206)				O(301)	2.58
P2′ (Ile)	N(207)		O(127)			3.37
	O(207)		N(129)			3.40
P3′ (Val)	N(208)		O(148)			2.86
	O(208)		N(148)			3.44
	OXT(208)				O(395)	2.48

Table V: Close Contacts in the Active Site

OS(P1)···OD1(Asp25)	2.41 Å
OS(P1)···OD2(Asp25)	2.87 Å
OS(P1)···OD1(Asp125)	3.07 Å
OS(P1)···OD2(Asp125)	2.72 Å
OD1(Asp25)···OD1(Asp125)	2.79 Å
N(Gly27)···OD1(Asp25)	3.28 Å
N(Gly127)···OD1(Asp125)	2.78 Å
N(Thr126)···OG1(Thr26)	3.01 Å
N(Thr26)···OG1(Thr126)	3.15 Å
OG1(Thr26)···O(Leu124)	2.94 Å
OG1(Thr126)···O(Leu24)	2.48 Å
N(Ala28)···O(Asp25)	3.51 Å
N(Ala128)···O(Asp125)	2.68 Å
N(P1)···O(Gly27)	3.51 Å
N(P2′)···O(Gly127)	3.37 Å
O(Thr26)···O(Wat305)	3.24 Å
O(Gly27)···O(Wat358)	2.44 Å
O(Gly127)···O(Wat304)	2.95 Å

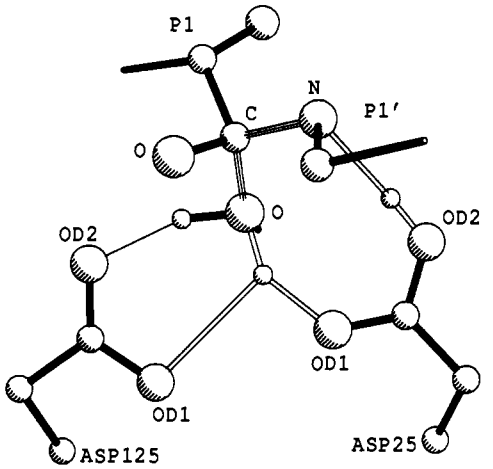

FIGURE 9: Catalytic mechanism proposed in this paper. Open lines represent H bonds in transition. Triple lines represent covalent bonds that are being formed/broken. The skeleton of the substrate and the aspartate side chains are at identical positions as the corresponding atoms in the present structure, the attacking water molecule has been placed at the Oσ(205) position of the present inhibitor and the "carbonyl" O atom completes the tetrahedral geometry at C(205). The small circle near the attacking water molecule indicates the position of the active-site water molecule in the native RSV PR structure (Miller et al., 1989a; Jaskólski et al., 1990) after least-squares alignment of the active sites of these two proteases.

similar to those identified in two other HIV-1 PR–inhibitor complexes (Miller et al., 1989b; Swain et al., 1990).

An intriguing feature of the inhibitor binding in the active site is the presence of a water molecule (Wat301) between the inhibitor and the flaps (Figure 5). This water molecular has been found in all retrovial PR–inhibitor complexes studied by X-ray crystallography (Miller et al., 1989b; Swain et al., 1990; Erickson et al., 1990; Fitzgerald et al., 1990), whereas it has not been observed in the inhibitor complexes of pepsin-like proteases. This water molecule has a very well-defined $2|F_o| - |F_c|$ density (Figure 7), which corresponds to the highest peak in the $|F_o| - |F_c|$ map. Consequently, there is no doubt about the precise location of Wat301 in the present complex. This water molecule is locked in its position with four H bonds having a nearly perfect tetrahedral arrangement (Table III). It accepts two H bonds from the amide N atoms of the isoleucine residues in the flaps (Ile50 and Ile150) and donates two H bonds to the main-chain carbonyl O atoms of residues P2 and P1′ of the inhibitor (Figure 5). Those two carbonyl groups are the closest C=O neighbors of the scissile bond analogue in the inhibitor molecule. Figure 5 illustrates that the short H bonds between Wat301 and those carbonyl O atoms (Table III) promote the deformation around the CHOH–CH_2 bond in the central part of the inhibitor molecule and thus facilitate the projection of the OH group toward the catalytically essential Asp25 and Asp125 side-chain carboxyls. If, as these inhibitor studies suggest, Wat301 is also present in the active site when a substrate is bound there, it would be rather unlikely for it to take an active part in the proteolytic mechanism (e.g., as a nucleophile) due to its relatively long distance from the scissile bond (>3.5 Å). On the other hand, it could serve a mechanical role in forcing the scissile bond toward the conformation required for hydrolysis, thus reducing the double-bond character and accelerating the reaction by a "strain" mechanism (Jencks, 1969).

The absence of Wat301 in inhibitor/substrate-bound pepsin-like proteases would be another point of difference between these two classes of aspartic proteases. The reason for this absence lies most probably in the fact that pepsin-like aspartic proteases have only one flap arm, which is not sufficient to secure analogous water molecule in this site (Gustchina & Weber, 1990). On the other hand, a mediating water molecule may not be necessary in the case of cellular aspartic proteases, where the tip of the single flap can reach closer to the inhibitor without being locked by a complementary flap.

Further, direct interactions between the inhibitor and the flaps include main-chain H bonds with residues Gly48 and Gly148 (Table IV). Gly48 forms a one-segment parallel β sheet with residues P4/P2 while Gly148 forms a one-segment antiparallel β sheet with P3′. On the average, therefore, β-sheet interactions between the inhibitor and the flaps are formed three residues away from the scissile bond position. On its active-site face, the inhibitor is also involved in β-sheet interactions with the enzyme. Residue P2′ forms a one-segment parallel β sheet with Gly127 and Asp129, while residues P3 and P1 are involved in incomplete antiparallel β-sheet interactions with Asp29 and Gly27 (Figure 5, Table IV). Thus, the inhibitor forms β sheets with the active-site floor of the catalytic cavity at positions that are, on the average, two residues away from the scissile bond replacement. Such

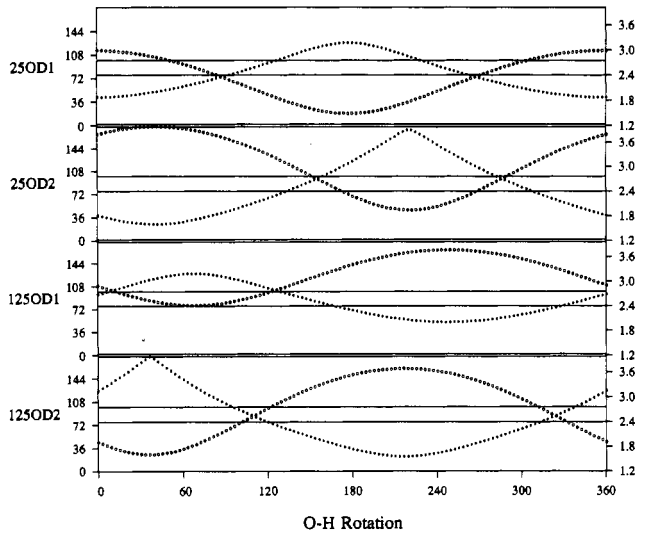

FIGURE 10: H···O distances (Å, open circles) and O–H···O angles (deg, full circles) between the C–OH hydroxyl donor of the inhibitor and the carboxyl O atoms of the active-site aspartates as a function of O–H rotation (deg) around the inhibitor C–OH bond. H bond formation criteria [H···O < 2.4 Å (Hamilton, 1968) and O–H···O > 104° (Jaskólski, 1984)] are marked by horizontal lines.

a distribution of main-chain H bonds with residues forming the catalytic cavity may be another factor responsible for the bending of the inhibitor molecule (see above).

The hydroxyl group of the scissile bond replacement (Ψ-[CH(OH)CH_2]) projects from the inhibitor main chain to a position between the carboxylic side-chain groups of the active-site aspartates (Figure 5). The H-bond network within the active site (Table V) is unchanged from that found in an uncomplexed retroviral protease (Miller et al., 1989a; Jaskólski et al., 1990; Wlodawer et al., 1989). In particular, the inner O atoms of the aspartates are within H-bonding distance and both make H bonds with the catalytic-triplet glycines in their own loops, and there is the "fireman's grip" H-bonding network between Thr26 and Thr126, which, in addition to the interaction between the aspartates, is the major element in the active-site architecture. The OH group of the inhibitor occupies the same position between the carboxylic groups of the aspartates as the water molecule that is found in the active site of all uncomplexed aspartic proteases. Figure 9 shows the position of the OH group of the present inhibitor and of the water molecule in the native RSV PR structure after least-squares alignment of the active sites of these two enzymes.

It is generally believed that this water molecule, located between the active-site aspartates, acts as the nucleophile in hydrolysis of the peptide bond (Suguna et al., 1987). If the OH group in the present *S* diastereomer of the inhibitor represents the nucleophilic water molecule during hydrolysis of the peptide bond, then the fourth substituent on the scissile bond analogue C atom (H in this case) would represent the position of the original carbonyl O atom at the tetrahedral transition state. Therefore, if an inhibitor complex could be crystallized by using an optically pure *R* diastereomer, its OH group would probably not interact with the active-site aspartates but would mimic the behavior of the original carbonyl O atom during the course of the cleavage reaction. The OH group in the present complex is within H-bonding distance from all four O atoms of the aspartates (Table V). All those distances cannot, of course, represent H bonds from the C–OH donor. In order to check the H-bonding possibilities of the C–OH donor, the H position was calculated with standard geometry and the O–H bond was rotated around the C–O vector to identify those positions at which the O–H···O contacts fulfill the geometric criteria of an H bond (Hamilton, 1968; Jaskólski, 1984). The results are shown in Figure 10 and indicate that the C–OH donor on the inhibitor cannot form proper H bonds with both aspartates at the same time, although it can form bifurcated H bonds with each of the aspartates. This result is practically unchanged when the O–H distance is varied from 0.97 to 1.20 Å.

The important consequence is that one of the aspartates (the one that does not accept the C–O–H···O bond) must be protonated in order to bind to the inhibitor hydroxyl group. The outer O atom is more likely to be protonated since locating the proton on the inner, OD1, atom would require the other OD1 atom to accept three H bonds (OD1′–H···OD1, from Gly27 and from C–OH). This simple argument provides indirect evidence that the acidic proton that is believed to be present in the active site of all native aspartic proteases is also present in the inhibitor complex. The same result was obtained when the above analysis was carried out for the hydroxyethylamine inhibitor (JG-365) complexed with HIV-1 PR (Jaskólski, unpublished results).

From the accumulated structural data on retroviral proteases and their inhibitor complexes one can try to address the question of their catalytic mechanism or of the mechanism of action of aspartic proteases in general. Several mechanisms of action based on the crystallographic structures of free and inhibitor-complexed aspartic proteases have been proposed to date [e.g., Kay (1985), James et al. (1985), Pearl (1987), and Suguna et al. (1987)]. Modeling the proteolytic reaction pathway requires addressing several questions, some of which are (i) where is the acidic proton located in the free enzyme? (ii) what is the nature of the electron density peak found between the active-site aspartates of all free aspartic proteases? (iii) how is the scissile bond carbonyl group oriented in the active site when the substrate is locked in the catalytic cleft? and (iv) where is the attacking nucleophile?

A direct answer to question i cannot come from macromolecular X-ray crystallography since proton locations are not resolved by that technique. However, an indirect argument, like the one used above for the present complex, can be used to deduce the most probable location of the proton. As another example, the acidic proton can be deduced to bridge the inner aspartate O atoms in the complex between HIV-1 PR and a reduced-peptide inhibitor (Miller et al., 1989b). In that case there is no inhibitor hydroxyl group to penetrate between the carboxylate groups nor is any electron density peak found between the aspartates. They form a very short OD1···OD1′ contact of 2.6 Å requiring an H atom to bridge them. It should be noted here that, in variance with some schematic presentations, the proton in that bridge would not be located along the OD1···OD1′ line but would rather form an angular contact similar to that illustrated in Figure 9, which would both satisfy the directions of the O atoms orbitals and provide acceptable angles between the bridge H bond and the H bond to Gly27 at the OD1 atoms. These two examples indicate that the proton does not have to reside at one location in all situations but will rather change its attachment in response to changes in the environment.

The problem of the location of the acidic proton in an uncomplexed enzyme is closely related to the role of the water molecule in the active site. Retroviral proteases provide a better model here because in symmetrical environments they are truly symmetric (Wlodawer et al., 1989). The most likely role for the water molecule in this symmetric situation would be to place one of its O–H bonds along the dimer 2-fold axis to form a bifurcated H bond with both inner carboxylic O

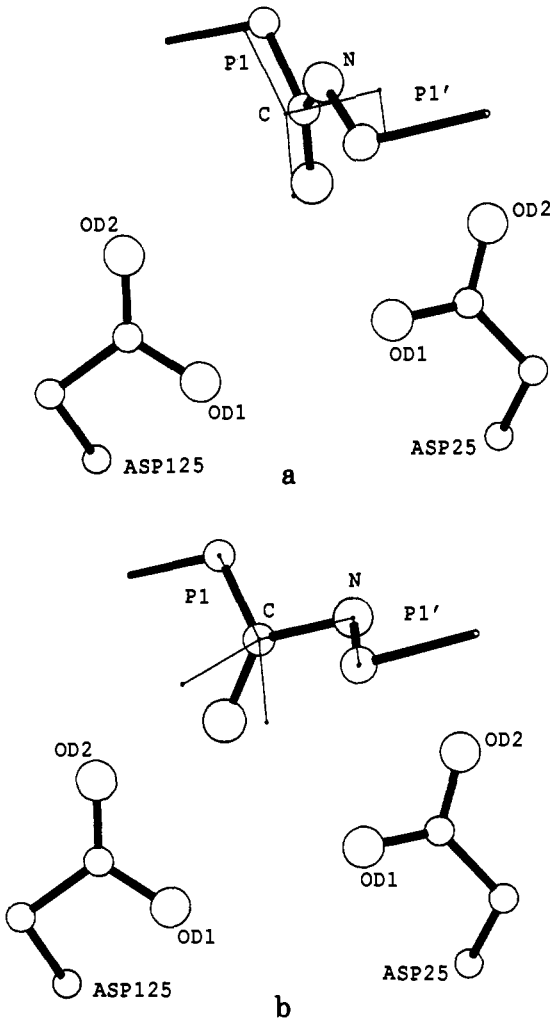

FIGURE 11: Fitting a substrate to the coordinates of the present inhibitor (thin lines). (a) Main chain fixed at P5–P2 and P2′–P3′; (b) main chain fixed at P1–P1′.

atoms and to use the other O–H bond to bind one of the outer OD2 atoms. The acidic proton would form an H bond to the water molecule from the other OD2 atom. A movement of the protons in the short OD2···H···Wat bridges would make the active site dynamically symmetric. A more extensive dynamic picture would even distribute the acidic proton over all four carboxylate O atoms. Perturbation of this symmetry, for instance by an approaching substrate/inhibitor molecule, could lock the dynamical equilibrium in one state. In the mechanism presented in Figure 9 the active-site water nucleophile starts its attack on the carbonyl C atom of the approaching substrate and leaves the acidic proton at OD2 of Asp25. At this location the acidic proton is in H-bonding position with the scissile amide N atom promoting its pyramidalization and thus weakening the peptide bond. As the attack of the nucleophile progresses, the carbonyl C atom's configuration drifts toward sp^3, the carbonyl bond becomes increasingly polarized, and the amide bond loses its double-bond character and lengthens. The nucleophilic attack on the C atom and the electrophilic attack on the N atom progress now in a concerted manner with the N···H–OD2 interaction becoming N–H···OD2. On the nucleophilic end, the formation of the new C–OH bond is accompanied by a weakening of the water O–H bond involved in the bridging interactions with the OD1 atoms. This former covalent O–H bond loses its covalent character and becomes a weakening H bond, which finally leaves the acidic proton in the bridge between the inner carboxylic O atoms. As the new N–H and C–OH bonds are being formed, the amide C–N bond weakens and breaks. Finally, the weakening H bonds between the cleaved products and the catalytic aspartates are broken and the carboxylic and amino products separate from the active site. The carboxylic groups of the active-site aspartates are held together by the inner OD1···H···OD1′ bridge and are ready to trap a new water molecule.

This catalytic mechanism shares common features with that proposed by Suguna et al. (1987) but there are also important differences. First of all, the cleavage process is an essentially one-step reaction in which the attacks of the nucleophile (water molecule) and the electrophile (acidic proton) are synchronized. Second, the postreaction catalytic aspartates are still bound by the acidic proton, which now resides between the inner O atoms. Third, at the beginning of the reaction the acidic proton is located on the OD2 atom of that aspartate, which is proximal to the N atom of the approaching amide. Suguna et al. (1987) placed this proton on the other aspartate, arguing that by H bonding to the scissile amide O atom it would promote its polarization. While the electronic effect of such an interaction would indeed favor the progress of the reaction, its geometrical effect would be to pull the C=O bond toward the active site, whereas the pyramidalization of the C atom requires just the opposite.

The mechanistic proposition presented above as well as most alternative models assumes that the attacking nucleophile is the active-site water molecule found in native aspartic proteases (Suguna et al., 1987). This picture of the proteolytic mechanism requires that the OH group of the present and any similar inhibitor be interpreted as a model of the attacking nucleophile. A different opinion holds that this hydroxyl represents the O atom of the original peptide group (James et al., 1985). To analyze this question we carried out two modeling experiments in which a real octapeptide was fitted to the coordinates of the inhibitor in the active site. First, the main-chain atoms of residues P5–P2 and P2′–P3′ were fixed at the inhibitor coordinates and the geometry of the P1–P1′ link was regularized. The result (Figure 11a) showed that the carbonyl C=O group would indeed point toward the active site matching the C–OH bond of the inhibitor. In this model, however, the strain that is clearly visible in the deformed geometry of the scissile dipeptide (Table II) has been completely lost because the scissile dipeptide assumed its relaxed conformation. In the second experiment, the modeled octapeptide substrate was fitted in the active site with the coordinates for the P1–P1′ dipeptide chain fixed as in the inhibitor (Figure 11b). Obviously, in this case the C=O group of P1 is just the bisector of the H–C–OH angle at the inhibitor and will be easily deformed to assume the orientation of C–H if the attacking water molecule comes from the HO–C direction.

In addition to the above arguments, the hypothesis that the active-site water is the nucleophile has the appeal of natural simplicity. This water molecule is central and unique in the structure of native aspartic proteases and by its H bonding in the active site it is naturally promoted as a nucleophile. It also has the most straightforward access from a nearly normal direction to the scissile peptide plane if the substrate carbonyl C atom is even slightly pyramidalized over the active site. On the other hand, the C=O oxygen atom placed between the carboxylic groups as the aspartates would have very limited possibilities of H bonding and would be immobilized, thus preventing effective pyramidalization of the C atom. Finally, there would have to be a specific water molecule promoted as a nucleophile that would have to find a way to attack the

peptide plane along its normal, which in the closely packed active-site cavity might be impossible to attain.

References

Blumenstein, J. J., Copeland, T. D., Oroszlan, S., & Michejda, E. J. (1989) *Biochem. Biophys. Res. Commun. 163*, 980–987.

Blundell, T. L., Cooper, J., Foundling, S. I., Jones, D. M., Atrash B., & Szelke, M. (1987) *Biochemistry 26*, 5585–5590.

Darke, P. L., Nutt, R. F., Brady, S. F., Garsky, V. M., Ciccarone, T. M., Leu, C.-T., Lumma, P. K., Freidinger, R. M., Veber, D. F., & Sigal, I. S. (1988) *Biochem. Biophys. Res. Commun. 156*, 297–303.

Dreyer, G. B., Metcalf, B. W., Tomaszek, T. A., Jr., Carr, T. J., Chandler, A. C., Hyland, L., Fakhoury, S. A., Magaard, V. W., Moore, M. L., Strickler, J. E., Debouck, C., & Meek, T. D. (1989) *Proc. Natl. Acad. Sci. U.S.A. 86*, 9752–9756.

Erickson, J., Neidhart, D. J., VanDrie, J., Kempf, D. J., Wang, X. C., Norbeck, D., Plattner, J. J., Rittenhouse, J., Turon, M., Wideburg, N., Kohlbrenner, W. E., Simmer, R., Helfrich, R., Paul, D., & Knigge, M. (1990) *Science 249*, 527–533.

Finzel, B. C. (1987) *J. Appl. Crystallogr. 20*, 53–55.

Fitzgerald, P. M. D., McKeever, B. M., VanMiddlesworth, J. F., Springer, J. P., Heimbach, J. C., Leu, C.-T., Herber, W. K., Dixon, R. A. F., & Darke, P. L. (1990) *J. Biol. Chem. 265*, 14209–14219.

Greenlee, W. J. (1990) *Med. Res. Rev. 10*, 173–236.

Gustchina, A., & Weber, I. T. (1990) *FEBS Lett. 269*, 269–272.

Hamilton, W. C. (1968) in *Structural Chemistry and Molecular Biology* (Rich, A., & Davidson, N., Eds.) pp 466–483, W. H. Freeman, San Francisco.

Hendrickson, W. (1985) *Methods Enzymol. 115*, 252–270.

James, M. N. G., Sielecki, A. R., & Hofmann, T. (1985) in *Aspartic Proteinases and Their Inhibitors* (Kostka, V., Ed.) pp 163–178, de Gruyter, Berlin.

Jaskólski, M. (1984) *Pol. J. Chem. 58*, 955–957.

Jaskólski, M., Miller, M., Rao, J. K. M., Leis, J., & Wlodawer, A. (1990) *Biochemistry 29*, 5889–5898.

Jencks, W. P. (1969) in *Catalysis in Chemistry and Enzymology*, pp 294–308, McGraw-Hill, New York.

Jones, A. (1985) *Methods Enzymol. 115*, 157–171.

Kay, J. (1985) in *Aspartic Proteinases and Their Inhibitors* (Kostka, V., Ed.) pp 1–17, de Gruyter, Berlin.

Kohl, N. E., Emini, E. A., Schleif, W. A., Davis, L. J., Heimbach, J. C., Dixon, R. A. F., Scolnick, E. M., & Sigal, I. S. (1988) *Proc. Natl. Acad. Sci. U.S.A. 85*, 4686–4690.

Kramer, R. A., Schaber, M. D., Skalka, A. M., Ganguly, K., Wong-Staal, F., & Reddy, E. P. *Science 231*, 1580–1584.

Lapatto, R., Blundell, T., Hemmings, A., Overington, J., Wilderspin, A., Wood, S., Merson, J. R., Whittle, P. J., Danley, D. E., Geoghegan, K. F., Hawrylik, S. J., Lee, S. E., Scheld, K. G., & Hobart, P. M. (1989) *Nature (London) 342*, 299–302.

McQuade, T. J., Tomasselli, A. G., Liu, L., Karacostas, V., Moss, B., Sawyer, T. K., Heinrikson, R. L., & Tarpley, W. G. (1990) *Science 247*, 454–456.

Meek, T. D., Lambert, D. M., Dreyer, G. B., Carr, T. J., Tomaszek, T. A., Jr., Moor, M. L., Strickler, J. E., Debouck, C., Hyland, L. J., Matthews, T. J., Metcalf, B. W., & Petteway, S. R. (1990) *Nature (London) 343*, 90–92.

Miller, M., Jaskólski, M., Rao, J. K. M., Leis, J., & Wlodawer, A. (1989a) *Nature (London) 337*, 576–579.

Miller, M., Schneider, J., Sathyanarayana, B. K., Toth, M. V., Marshall, G. R., Clawson, L., Selk, L., Kent, S. B. H., & Wlodawer, A. (1989b) *Science 246*, 1149–1152.

Navia, M. A., Fitzgerald, P. M. D., McKeever, B. M., Leu, C., Heimbach, J. C., Herber, W. K., Sigal, I. S., Darke, P. L., & Springer, J. P. (1989) *Nature (London) 337*, 615–620.

Oroszlan, S. (1989) in *Viral Proteinases as Targets for Chemotherapy* (Krausslich, H. G., Oroszlan, S., & Wimmer, E., Eds.) pp 87–100, Cold Spring Harbor Press, Cold Spring Harbor, NY.

Pearl, L. (1987) *FEBS Lett. 214*, 8–12.

Peters, D., & Peters, J. (1981) *J. Mol. Struct. 85*, 107–123.

Ramachandran, G. N., & Sasisekharan, V. (1968) *Adv. Protein Chem. 23*, 283–437.

Rich, D. W., Green, J., Toth, M. V., Marshal, G. R., & Kent, S. B. H. (1990) *J. Med. Chem. 33*, 1285–1288.

Richards, A. D., Roberts, R., Dunn, B. M., Graves, M. C., & Kay, J. (1989) *FEBS Lett. 247*, 113–117.

Richards, A. D., Broadhurst, A. V., Ritchie, A. J., Dunn, B. M., & Kay, J. (1990) *FEBS Lett. 253*, 214–216.

Richardson, J. S. (1981) *Adv. Protein Chem. 34*, 167–339.

Roberts, N. A., Martin, J. A., Kinchington, D., Broadhurst, A. V., Craig, J. C., Duncan, I. B., Galpin, S. A., Handa, B. K., Kay, J., Kröhn, A., Lambert, R. W., Merrett, J. H., Mills, J. S., Parkes, K. E. B., Redshaw, S., Ritchie, A. J., Taylor, D. L., Thomas, G. J., & Machin, P. J. (1990) *Science 248*, 358–361.

Sawyer, T. K., Palas, D. T., Mao, B., Staples, D. J., deVaux, A. E., Maggiora, L. L., Affholter, J. A., Kati, W., Duchamp, D., Hester, J. B., Smith, C. W., Saneii, H. H., Kinner, J., Handschumacher, M., & Carlson, W. (1988) *J. Med. Chem. 31*, 18–30.

Schneider, J., & Kent, S. B. H. (1988) *Cell 54*, 363–368.

Sheriff, S. (1967) *J. Appl. Crystallogr. 20*, 55–57.

Smith, J. L., Corfield, P. W. R., Hendrickson, W. A., & Low, B. W. (1988) *Acta Crystallogr. A44*, 357–368.

Steigemann, W. (1974) Ph. D. Thesis, Technische Universität, München.

Suguna, K., Padlan, E. A., Smith, C. W., Carlson, W. D., & Davies, D. (1987) *Proc. Natl. Acad. Sci. U.S.A. 84*, 7009–7013.

Swain, A. L., Miller, M., Green, J., Rich, D. H., Schneider, J., Kent, S. B. H., & Wlodawer, A. (1990) *Proc. Natl. Acad. Sci. U.S.A. 87*, 8805–8809.

Tomasselli, A. G., Hui, J. O., Sawyer, T. K., Staples, D. J., Bannow, C., Reardon, I. M., Howe, W. J., DeCamp, D. L., Craik, C. S., & Heinrikson, R. L. (1990a) *J. Biol. Chem. 265*, 14675–14683.

Tomasselli, A. G., Olsen, M. K., Hui, J., Staples, D. J., Sawyer, T. K., Heinrikson, R. L., & Tomich, C.-S. C. (1990b) *Biochemistry 29*, 264–269.

Wlodawer, A., Miller, M., Jaskólski, M., Sathyanarayana, B. K., Baldwin, E., Weber, I. T., Selk, L. M., Clawson, L., Schneider, J., & Kent, S. B. H. (1989) *Science 245*, 616–621.

Wuts, P. G. M., Putt, S. R., & Ritter, A. R. (1988) *J. Org. Chem. 53*, 4503–4508.